

Development of an HV-CMOS active pixel sensor "AstroPix" for all-sky medium-energy gamma-ray telescopes

Yusuke Suda,^{a,*} Regina Caputo,^b Amanda L. Steinhebel,^b Henrike Fleischhack,^{b,c,d} Nicolas Striebig,^e Manoj Jadhav,^f Ricardo Luz,^f Daniel Violette,^b Carolyn Kierans,^b Hiroyasu Tajima,^g Yasushi Fukazawa,^a Richard Leys,^e Ivan Peric,^e Jessica Metcalfe,^f Michela Negro^{b,d} and Jeremy S. Perkins^b

^a*Physics Program, Graduate School of Advanced Science and Engineering, Hiroshima University,
739-8526 Hiroshima, Japan*

^b*NASA Goddard Space Flight Center, Greenbelt, MD, USA*

^c*Catholic University of America, 620 Michigan Ave NE, Washington, DC 20064, USA*

^d*Center for Research and Exploration in Space Science and Technology, NASA/GSFC, Greenbelt, MD
20771, USA*

^e*ASIC and Detector Laboratory, Karlsruhe Institute of Technology, Karlsruhe, Germany*

^f*Argonne National Laboratory, Lemont, IL 60440, USA*

^g*Institute for Space-Earth Environmental Research and Kobayashi-Maskawa Institute for the Origin of
Particles and the Universe, Nagoya University, Japan*

E-mail: ysuda@hiroshima-u.ac.jp

All-sky medium-energy gamma-ray observations are essential to deepen our understanding of physics in extreme astronomical objects such as gamma-ray bursts and active galactic nuclei. Those observations are also highly needed to further develop multi-messenger astronomy. Next-generation all-sky MeV gamma-ray telescopes must have a large area detector and keep high sensitivities even in the energies in which Compton scattering is dominant. Having both a silicon tracker (scatterer) and a calorimeter (absorber) as the main detector is a promising configuration for such a space mission. In order to fulfill the requirements such as a large sensitive area, low noise, high energy/positional resolution, and low power, we have been developing an HV-CMOS active pixel sensor, AstroPix. In this contribution, we report performance evaluations of AstroPix such as I-V and noise, energy calibration/resolution/threshold, and depletion depth measurements. Current achievements as a sensor for next-generation all-sky MeV gamma-ray telescopes and future development will be discussed.

38th International Cosmic Ray Conference (ICRC2023)
26 July - 3 August, 2023
Nagoya, Japan



*Speaker

1. Introduction

Medium-energy (MeV) gamma-ray observations provide essential ingredients to understand physics in high energy astronomical phenomena such as gamma-ray bursts (GRBs), active galactic nuclei (AGNs), and so on. Since GRBs and AGN flares happen at any direction in the Universe, all-sky MeV gamma-ray monitoring with a good localization capability will play an essential role in multi-messenger astronomy.

MeV photons interact with material mainly via Compton scattering (the year 2023 is the 100th anniversary of its discovery by A. Compton). The detector thus requires to capture both a recoil electron and scattered photon and to record their hit positions and energies. Since the angular resolution is primarily given by both the energy and positional resolution of the detector, a wide field of view detector with a capability of precise position and energy determination is desired for a future all-sky MeV gamma-ray mission. Various types of detectors have been proposed, but none of them is founded yet as of today.

The All-sky Medium Energy Gamma-ray Observatory eXplorer (AMEGO-X) is one of the future MeV mission candidates [1]. Its gamma-ray telescope has a 2π sr field of view (< 10 MeV) and the localization accuracy of 1° (90% CL radius) for transient phenomena. The gamma-ray detector of the telescope consists of four identical stacked silicon tracker towers and requires $\sim 6 \times 10^4$ cm 2 silicon area. Given the limited power resource of satellite, AMEGO-X demands a low power and low noise pixel silicon sensor with high positional and energy resolutions.

We have been developing a new type of silicon pixel sensor, AstroPix, for AMEGO-X. We report the overview of the development, the basic performance of the second version (V2) of AstroPix, the status of the third version (V3), and the future prospect.

2. AstroPix

AstroPix is a newly developed monolithic high voltage CMOS (HV-CMOS) active pixel sensor based on the experience of the developments of both ATLASpix and MuPix [2]. Fig. 1 shows the schematic diagram of AstroPix. By applying an HV, the sensor layer can be fully depleted.

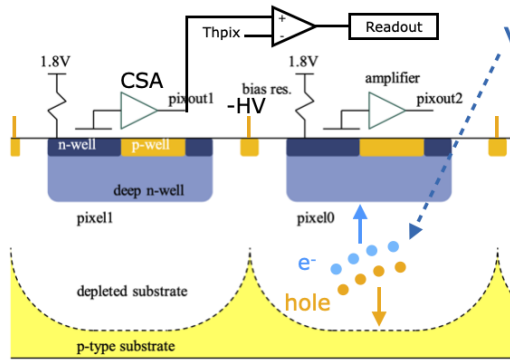


Figure 1: Schematic diagram of AstroPix. From I. Peric [3] with modifications

The electrons created via a gamma-ray interaction in the depletion volume are collected by the

28 n-well. The signal is processed on the pixel through a charge sensitive amplifier and comparator
 29 for the pixel-level trigger ("hit"). Finally the time-over-thresholds (ToTs) from all the hit pixels are
 30 digitized in the periphery of the chip. Therefore, both the power consumption and noise (thanks to
 31 on-chip signal-processing and digitization) in AstroPix are expected to be low and a high capability
 32 of gamma-ray detection (thanks to a large depletion volume) can be achieved.

33 The requirements for AstroPix to be adopted by AMEGO-X are listed in Table 1. The first
 34 version of AstroPix (V1) chip is $725 \mu\text{m}$ thick and contains 18×18 pixels whose pixel pitch is
 35 $175 \times 175 \mu\text{m}^2$. It was used to understand the sensor and to develop the data acquisition (DAQ)
 36 tools. The power consumption is 14.7 mW/cm^2 and the emission lines from radioisotopes ranging
 37 from 14 keV to 122 keV can be found in the analog data [4]. However, the digital data readout is
 38 not available due to a flaw in the chip design.

Table 1: Requirements for AstroPix

| | | | |
|--|------------------|-------------------------|-----------------|
| Pixel pitch (μm^2) | 500×500 | Dynamic range (keV) | 25 - 700 |
| Thickness (μm) | 500 | Energy resolution (keV) | 5 (1σ) |
| Power consumption (mW/cm^2) | 1.5 | | |

38
 39 The AstroPix V2 chip is $725 \mu\text{m}$ thick and contains 35×35 pixels whose pixel pitch is
 40 $250 \times 250 \mu\text{m}^2$. The most important upgrade from V1 is the capability of recording the digital data,
 41 it is now possible to readout ToT value from each pixel over the chip. The analog data can be read
 42 only from the first row pixels. The power consumption is 3.4 mW/cm^2 .

43 3. Performance of AstroPix V2

44 In this section, we report results from V2 chips from a $(300 \pm 100) \Omega \cdot \text{cm}$ resistivity wafer.
 45 The nominal operating bias voltage is -160 V supplied by KEITHLEY 2450 SourceMeter.

46 3.1 I-V curve and typical waveform

47 The bias voltage dependence of the current draw in a V2 chip was measured by KEITHLEY
 48 2450 SourceMeter as shown in Fig. 2. The breakdown was observed when the bias voltage reached
 49 at around -190 V .

50 Fig. 3 shows a typical waveform outputted from the charge sensitive amplifier in an analog pixel
 51 when irradiated by ^{109}Cd (22.2 keV), which was measured by an oscilloscope (LeCroy T3DSO2302).

52 3.2 Energy spectra and calibration

53 By accumulating waveforms with various radioisotopes, the energy spectra in pulse height
 54 were measured as shown in Fig. 4. The emission lines ranging from 13.9 keV to (122.1 - 136.5) keV
 55 and the Compton edge corresponding to (122.1 - 136.5) keV photons can be found. Fig. 5 shows
 56 the correlation between the true energies and the measured pulse heights, showing a good linearity
 57 up to $\sim 80 \text{ keV}$ where the analog output starts to saturate due to the saturation in the output buffer
 58 for analog data.

59 Energy spectra in ToT (digital output) are shown in Fig. 6. Because of the limitation of the
 60 ToT counter bits, the ToT value of $20.48 \mu\text{s}$ is the upper edge of the dynamic range in the current

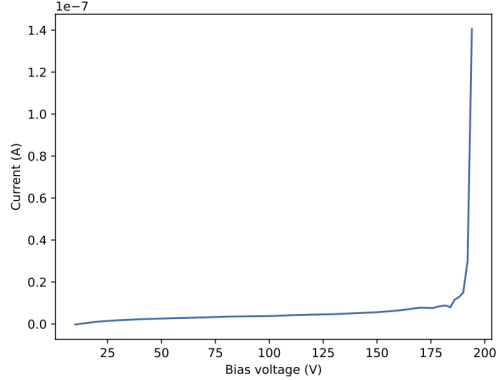


Figure 2: I-V curve. The breakdown voltage is around -190 V.

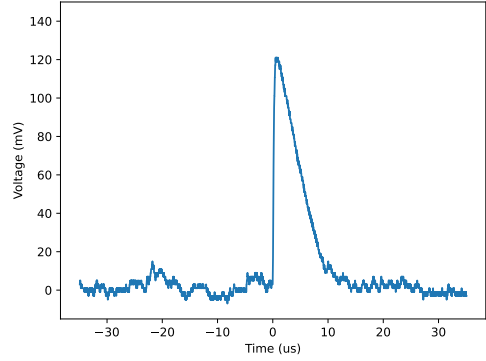


Figure 3: Typical waveform from a pixel when irradiated by ^{109}Cd .

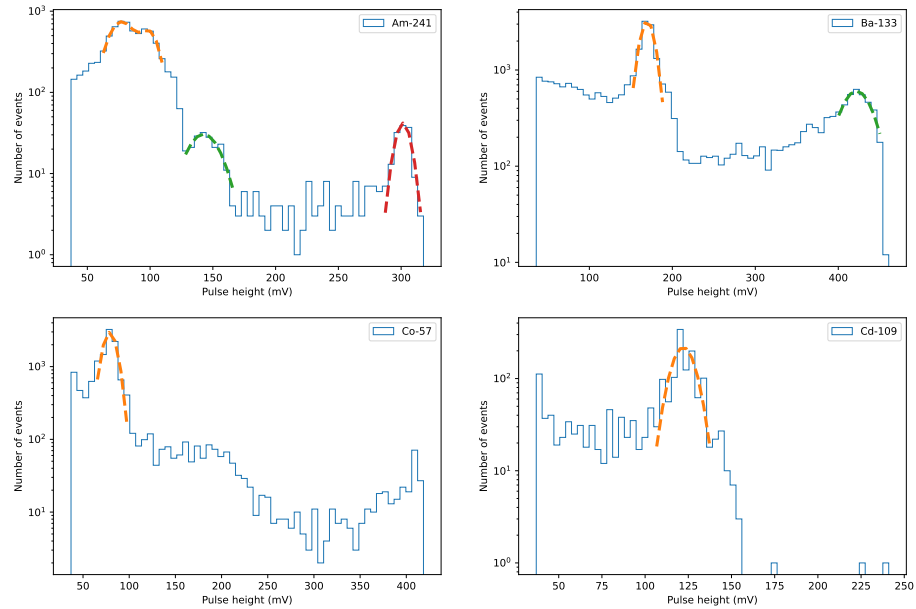


Figure 4: Energy spectra in pulse height from a pixel. *Top left:* ^{241}Am (the photopeaks of 13.9 keV and 17.8 keV fitted with a double Gaussian in orange, 26.3 keV fitted with a Gaussian in green, and 59.5 keV fitted with a Gaussian in red). *Top right:* ^{133}Ba (31.0 keV in orange and 81.0 keV in green). *Lower left:* ^{57}Co (14.4 keV in orange, the Compton edge around 200 mV, and (122.1 - 136.5) keV around 400 mV). *Lower right:* ^{109}Cd (22.2 keV in orange).

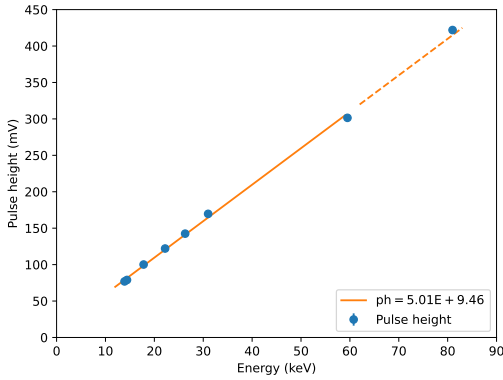


Figure 5: Energy calibration in pulse height for a pixel. The photopeaks from 13.9 keV to 59.5 keV were used to fit by a linear function. The fitted values are shown in the legend. The dotted line is the extrapolation.

61 configuration. The photopeak of 81.0 keV is visible even though it was affected by the limitation
 62 of the ToT counter. Fig. 7 shows the energy calibration in the digital data and the comparison of
 63 the energy resolution between the digital and analog data. The linearity can be seen until around
 64 ~ 80 keV as well. The energy resolutions in digital are comparable to those in analog and basically
 satisfy the requirement at least in this pixel.

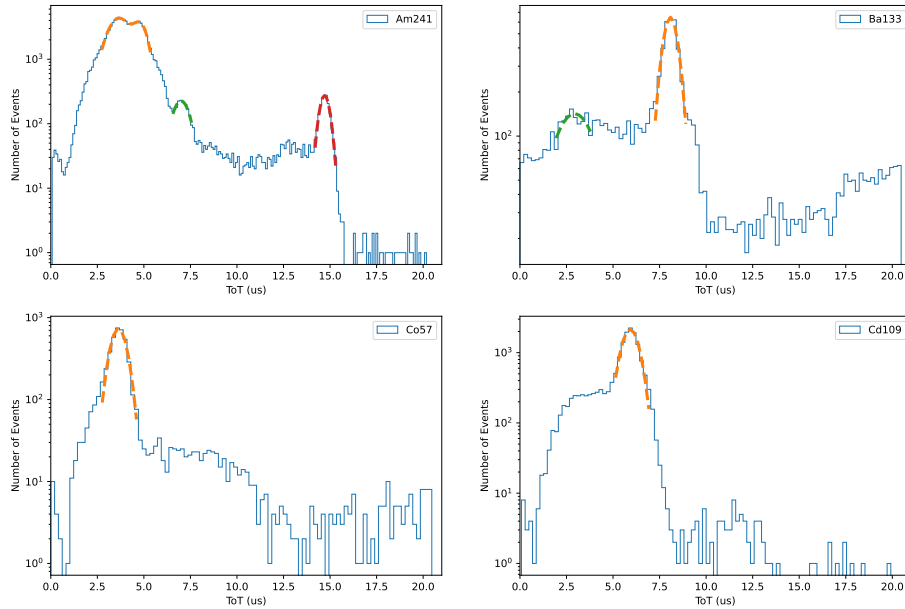


Figure 6: Energy spectra in ToT from a pixel. The notations are the same as in Fig. 4.

65

66 3.3 Noise map

67 To evaluate overall noise distribution in the chip, hit rates were measured with various threshold
 68 voltages. Only one pixel was enabled to readout the digital data at a time in order to minimize

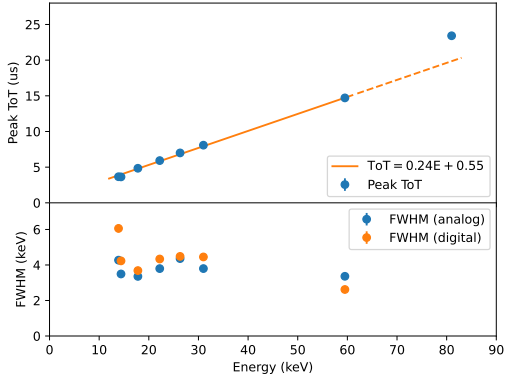


Figure 7: Energy calibration in ToT (*Top panel*) and energy resolutions (FWHM, *Lower panel*) for a pixel. The photopeaks from 13.9 keV to 59.5 keV were used to fit by a linear function. The fitted values are shown in the legend. The dotted line shows the extrapolated line. The FWHM points for analog were evaluated from the data measured by a multi-channel analyzer through a shaping amplifier.

69 the deadtime. The threshold upper limit is defined as the threshold value at which the rate (=
70 Number of hits/30 sec) becomes zero for the first time by looking from the lowest threshold (25 mV).
71 The resultant noise map and its population are shown in Fig. 8 and 9. The noise level differs from
72 pixel to pixel, but there is no clear pattern or structure over the chip. Assuming there is no gain
73 variation over the sensor, one can use the fitted parameters given in Fig. 5 to estimate the fraction
74 of pixels which satisfy the lower edge of the dynamic range (the corresponding voltage is 135 mV).
75 It is estimated that almost 90% of the pixels satisfy the requirement of 25 keV in the current
configuration.

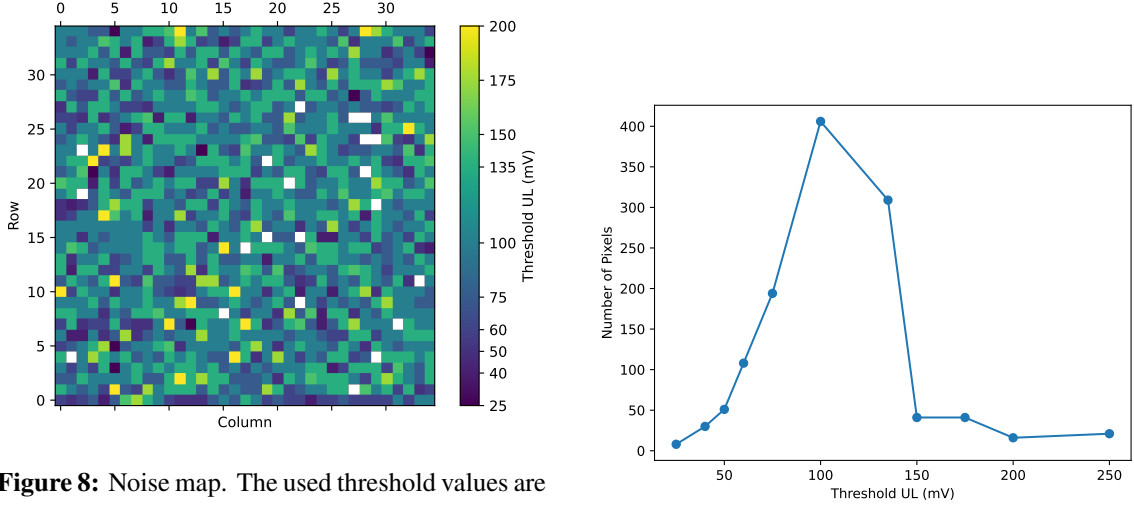


Figure 8: Noise map. The used threshold values are indicated in the color bar. The pixels in white have a larger threshold upper limit than 200 mV.

Figure 9: Noise population.

77 **3.4 Depletion depth**

78 The growth of the depletion layer in a pixel was evaluated as follows: 1. Measure the rate of
 79 59.5 keV photons coming from ^{241}Am located at a distance of 3 cm from the chip. 2. Scan the
 80 bias voltages and do the step 1 at each stage. 3. Calculate the depletion depth by using the rate,
 81 estimated photon intensity, and photoelectric cross section. 4. Compare the data with the simple
 82 theoretical PN junction model give by;

$$d = \sqrt{2\epsilon\mu\rho (V_{\text{bias}} + V_{\text{built_in}})} \quad (1)$$

83 where d is the theroretical depletion depth, ϵ the permittivity, μ the hole mobility, ρ resistivity, V_{bias}
 84 the bias voltage, and $V_{\text{built_in}}$ the built-in potential. Fig. 10 shows the growth curve of the depletion
 85 layer. Here, however, the data points are scaled to match the model since the detailed evaluation
 86 including systematic uncertainties is underway. Nevertheless, the obtained curve seems to follow
 87 the model, implying the depletion layer of the V2 chip grows as expected. In order to fully deplete,
 it is evident that we need to develop chip with a much higher resistivity.

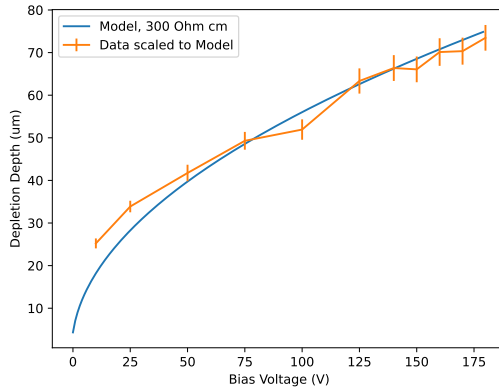


Figure 10: Growth curve of the depletion layer in a pixel. The data points are scaled to match the model.

88 With the similar setup, but inserting a Copper sheet between ^{241}Am and the sensor to make a
 89 single peak ToT distribution by eliminating lower energy photons, the depletion depth of almost all
 90 the pixels were evaluated (Fig. 11 and 12). The effective time was calculated by using the waiting
 91 time distribution. No clear pattern nor structure are visible and the deviation is 9%.

93 **4. AstroPix V3**

94 The AstroPix V3 chip, the first full reticle chip, is $725 \mu\text{m}$ thick and contains 35×35 pixels
 95 whose pixel pitch is $500 \times 500 \mu\text{m}^2$. While expanding the pixel pitch to the value that is required,
 96 the pixel size is kept as small as possible to reduce capacitance. The designed power consumption
 97 is 1 mW/cm^2 .

98 The basic performance evaluation is ongoing. Photopeaks from several radioisotopes were
 99 visible even though the noise level seem to get higher due to a larger pixel size compared to that in
 100 V2. The gain linearity was also confirmed by using the obtained peaks.

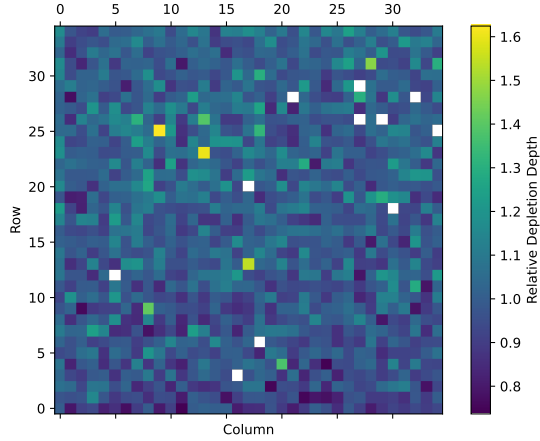


Figure 11: Depletion depth map. The pixels in white were too noisy to measure 59.5 keV photons. The different chip was used from the one in Fig. 8.

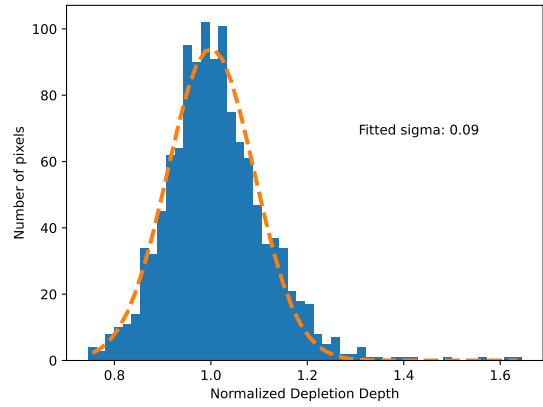


Figure 12: Normalized depletion depth distribution (1D projection of Fig. 11). The dotted line shows a Gaussian fit and the fitted sigma is 0.09.

101 5. Summary and outlook

102 Performance of AstroPix V2 was evaluated in both analog and digital. The dynamic range
 103 is from 13.9 keV (or less) to 80 keV. The gain linearity is confirmed up to 80 keV. The energy
 104 resolution basically satisfies the requirement. The depletion layer grows as expected, but not yet
 105 fully depleted. AstroPix V3 was developed to fulfill the requirements of the pixel pitch and the
 106 power consumption.

107 Towards the use of AstroPix in space, “Quad-chip”, a 2×2 array of V3 chips, is in preparation
 108 for testing. A Quad-chip will be mounted on a sounding rocket and be operated in space to increase
 109 the NASA’s technical readiness level [5].

110 Acknowledgments

111 This work is funded in part by 18-APRA18-0084. YS’s work was supported by JSPS KAKENHI
 112 Grant Number JP23K13127.

113 References

- 114 [1] R. Caputo *et al.*, “All-sky Medium Energy Gamma-ray Observatory eXplorer mission concept,” Journal of Astro-
 115 nomical Telescopes, Instruments, and Systems, 8, 4, 044003 (2022).
- 116 [2] I. Perić and N. Berger, “High Voltage Monolithic Active Pixel Sensors,” Nucl. Phys. News 28(1), 25–27 (2018).
- 117 [3] I. Perić, “Development of novel high-voltage CMOS sensor,” <https://adl.ipe.kit.edu/downloads/ThesisHVCmos.pdf>
- 118 [4] A. L. Steinhebel *et al.*, “AstroPix: novel monolithic active pixel silicon sensors for future gamma-ray telescopes,”
 119 Proc. SPIE 12181 (2022).
- 120 [5] A. L. Steinhebel *et al.*, “A-STEP for AstroPix: Development and Test of a space-based payload using novel pixelated
 121 silicon for gamma-ray measurement,” in these proceedings (2023).